

Remote sensing of the solar site of interchange reconnection associated with the May 1997 magnetic cloud

N. U. Crooker¹ and D. F. Webb²

Received 3 February 2006; revised 19 April 2006; accepted 2 May 2006; published 30 August 2006.

[1] The direction of suprathermal electron flux on open magnetic field lines in the 15 May 1997 magnetic cloud is used to predict the solar location of the interchange reconnection that released one end of what presumably were doubly connected field lines in the coronal mass ejection (CME) of origin on 12 May. A search for an X-ray signature of the interchange reconnection in the predicted location reveals a long-lasting arched structure stretching from high above the CME site to the northern polar coronal hole. At the edge of the coronal hole, coincident with the X-ray feature, are previously reported extreme ultraviolet brightenings (“crinkles”). The observations are consistent with a CME flux rope forming in a near-quadrupolar configuration while overhead open field lines reconnect with the rising, closed, rope fields to open one leg of the rope loop. The pattern is similar to the breakout model except there are no closed overhead field lines through which the rising flux rope must break out. The near-quadrupolar source appears to be responsible for the mismatch between the polarity of the flux rope observed at 1 AU and the sector in which it was embedded. Spacecraft interception of the leg rather than the apex of the flux rope loop may be responsible for the mismatch between the low inclination of the cloud axis and the high inclination predicted from the preexisting filament and magnetic configuration at the source.

Citation: Crooker, N. U., and D. F. Webb (2006), Remote sensing of the solar site of interchange reconnection associated with the May 1997 magnetic cloud, *J. Geophys. Res.*, *111*, A08108, doi:10.1029/2006JA011649.

1. Introduction

[2] Because of its spatial and temporal isolation from similar events, the magnetic cloud that engulfed Earth on 15 May 1997 and its eruption from the Sun in a coronal mass ejection (CME) on 12 May have been the subject of many coordinated studies and publications [e.g., *Plunkett et al.*, 1998; *Thompson et al.*, 1998; *Webb et al.*, 2000; *Arge et al.*, 2004; *Liu*, 2004; *Odstrcil et al.*, 2004, 2005; *Linker et al.*, 2005]. While the event’s isolation provided an opportunity to make clear associations between solar and in situ signatures, many aspects of the erupting CME remain poorly understood. Here we add to the body of knowledge about the May 1997 event some new information from in situ suprathermal electron measurements ($E > 80$ eV) that bear upon models of the configuration of magnetic reconnection back at the Sun.

[3] Since suprathermal electrons continually stream out from the Sun along magnetic field lines, they are commonly used as sensors of whether field lines are connected to the Sun at one or both ends, that is, whether field lines are open or closed. If connected at both ends, the electron distributions are bidirectional, or counterstreaming. While counter-

streaming electrons were one of the first signatures used to identify interplanetary coronal mass ejections (ICMEs) on a routine basis [e.g., *Gosling et al.*, 1987, 1990], it was soon recognized that not all fields in ICMEs are connected to the Sun at both ends. In particular, in those ICMEs classified as magnetic clouds [e.g., *Burlaga*, 1991], *Shodhan et al.* [2000] found that fields range from 100% open to 100% closed.

[4] Under the assumption that all field lines in CMEs are originally closed loops, the means by which they open is thought to be interchange reconnection, where an open field line reconnects with one leg of a large CME loop that is expanding into the heliosphere, thereby interchanging it for a small loop at the solar surface [*Gosling et al.*, 1995; *Crooker et al.*, 2002]. Which leg is the site of this interchange reconnection can be determined remotely from the direction of suprathermal electron flow relative to the magnetic field direction on any open field line in an ICME, since the electrons must be flowing from the leg that remains attached to the Sun. We apply this concept for the first time to the 15 May 1997 cloud. We predict where interchange reconnection occurred and find evidence in solar data that both support the prediction and provide information about the large-scale magnetic configuration of the CME site.

2. Analysis

[5] Wind data from the 15 May 1997 cloud were analyzed by *Webb et al.* [2000] and *Arge et al.* [2004]. Of

¹Center for Space Physics, Boston University, Boston, Massachusetts, USA.

²Institute for Scientific Research, Boston College, Chestnut Hill, Massachusetts, USA.

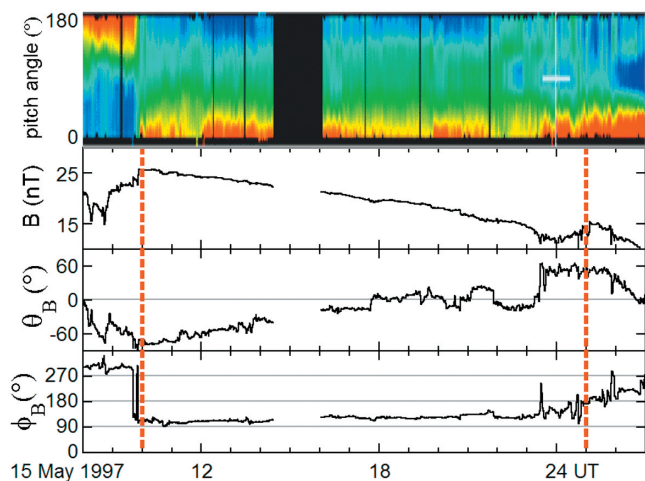


Figure 1. Time variations of color-coded (red is high intensity) electron pitch-angle distributions and magnetic field strength B , latitude angle θ_B , and longitude angle ϕ_B (GSE coordinates) from the Wind spacecraft as it passed through a magnetic cloud bounded by the red dashed vertical lines.

particular relevance here, they showed that the suprathermal electrons were unidirectional and streaming parallel to the magnetic field. Figure 1 illustrates these features in time variations of color-coded 260-eV electron pitch angle dis-

tributions from the 3DP instrument [Lin *et al.*, 1995] and of magnetic field parameters from the MFI magnetometer [Lepping *et al.*, 1995]. Between the dashed vertical lines marking the boundaries of the flux rope model fit to the cloud data by Webb *et al.* [2000], there is only a single red-yellow band of streaming electrons at 0° pitch angle, that is, parallel to the magnetic field. The lack of an accompanying band of counterstreaming electrons antiparallel to the field, at 180° , implies that all of the field lines in the cloud were open at 1 AU.

[6] The fact that the suprathermal electrons within the cloud were streaming parallel to the magnetic field means that the field lines on which they resided left the Sun with positive polarity, pointing away from the Sun, independent of any local inversions encountered by the spacecraft. In this case, Figure 1 shows that the magnetic field was not locally inverted, as it might be in some locations within the flux-rope structure of a magnetic cloud [e.g., Crooker *et al.*, 1998]. The magnetic longitude angle within the cloud pointed steadily away from the Sun at $\sim 110^\circ$, close to the positive-polarity Parker spiral direction of $\sim 135^\circ$, consistent with the positive polarity determined from the electron data.

[7] In the context of the large-scale magnetic sector structure in the heliosphere, the positive polarity of the cloud fields was opposite to the polarity of the sector in which the cloud was immersed, as pointed out by Arge *et al.* [2004]. This is contrary to the pattern in most interplanetary CMEs (ICMEs). Using the direction of the dominant

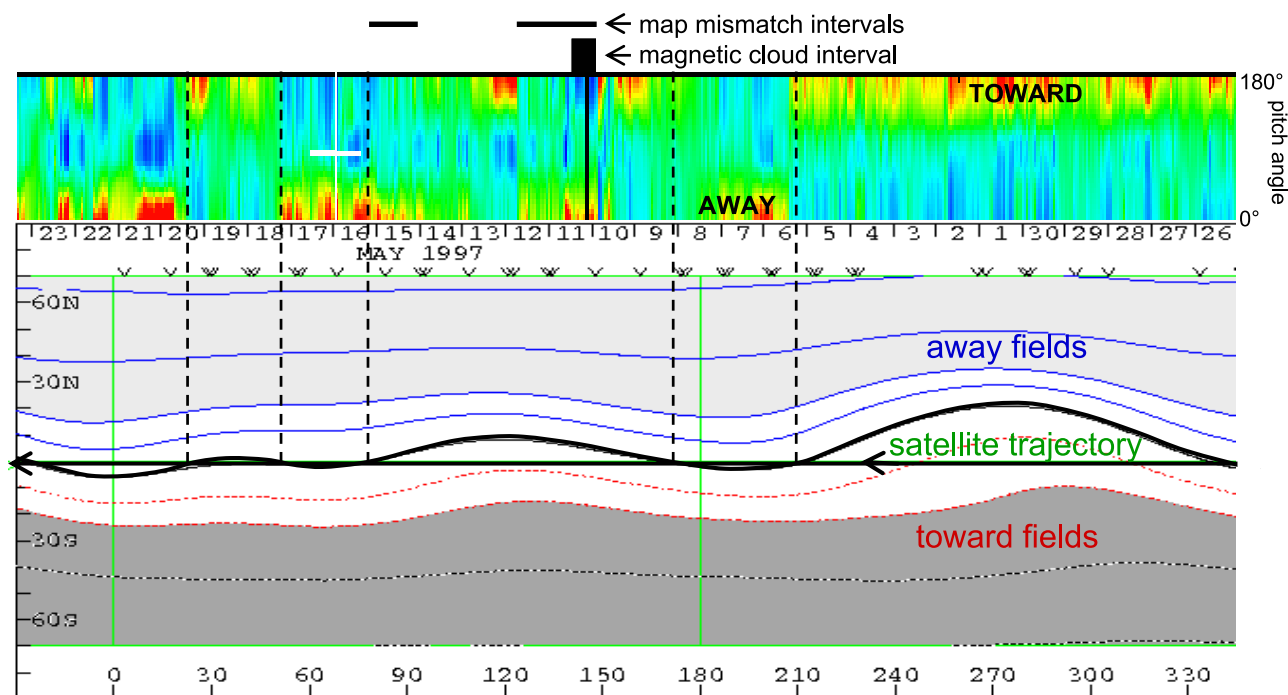


Figure 2. Time variations of color-coded electron pitch-angle distributions plotted from right to left to match the projected spacecraft passage across the potential field source surface map for Carrington Rotation 1922. The map was generated at the Wilcox Solar Observatory using the classic line-of-sight boundary condition and a source surface height of 2.5 solar radii. The contours of magnetic field strength lie at 0 (black curve), ± 1 , ± 2 , ± 5 , and ± 10 mT. Dashed vertical lines extending from trajectory intersections with the projected HCS at 0 mT mark predicted polarity changes.

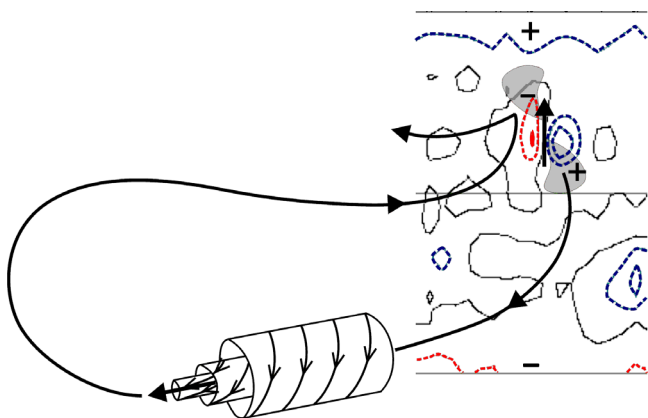


Figure 3. Schematic drawing of a magnetic cloud at 1 AU and its connection back to the solar surface, represented by a section of a photospheric field map from the Wilcox Solar Observatory for Carrington Rotation 1922 covering longitude 90° to 180° and latitude -70° to $+70^\circ$. The contours of magnetic field strength lie at 0 (black), ± 100 , and ± 200 mT, where the positive contours are blue and the negative red. The gray shapes approximate projected dimmings from EUV observations, and the vertical arrow represents the axis of the associated filament.

electron intensity in a counterstreaming event as an indicator of the polarity of which of the two legs of a closed ICME a spacecraft encounters, *Kahler et al.* [1999] showed that ICME legs are ten times more likely to match the polarity of the sector in which they are encountered than not. Although the study was confined to ICMEs with closed fields, presumably similar statistics apply to open-field ICMEs like the one of concern here. This polarity-matching property reflects the imprint of the dipolar component of the solar magnetic field [Crooker, 2000, 2005].

[8] Figure 2 illustrates how this polarity imprint was lacking for the May 1997 cloud. In the top panel, the color-coded electron pitch angle distribution plot for Carrington Rotation 1922 is shown with time running from right to left to match the pattern on the potential field source surface (PFSS) coronal map below it. To help compensate for the variable solar wind transit time from the Sun to the spacecraft in a simple, linear way, the pitch angle plot was displaced and uniformly stretched to maximize the match with polarity change predictions from the coronal map. The pitch angle plot covers ~ 26.6 days, beginning midday on 1 May and ending around 0200 UT on 28 May. Compared to the dates on the 28.4-day-long map, beginning on 26 April, the time lag of the pitch angle plot ranges from 5.5 days at the beginning to 3.7 days at the end, corresponding to transit speeds of 314 km/s and 466 km/s, respectively. The average observed speed of 361 km/s during the interval lies within that range, as expected. The predicted polarity changes lie at the vertical dashed lines marking the intersections of the projected trajectory of the Wind spacecraft with the heavy curve outlining the heliomagnetic equator, which traces the predicted projection of the heliospheric current sheet (HCS). These predicted polarity changes match the observed changes in the adjusted pitch

angle plot through most of the solar rotation. Where the satellite trajectory runs south of the HCS, starting from the right, the electron beam lies along the top of the plot, at 180° pitch angle, consistent with the predicted immersion in fields with toward polarity. As the trajectory crosses the HCS and passes above it at 210° longitude, the electron beam switches to 0° pitch angle, consistent with the predicted immersion in fields with away polarity. A similar match is present on the left end of the plot, even for the minor excursions above and beneath the predicted HCS. The only exceptions to the pattern lie within the sector containing the magnetic cloud, in the heliographic longitude interval $\sim 80^\circ$ – 170° . The electrons in two segments of that interval, the first containing the cloud itself, indicate polarity mismatches, as marked. They indicate away polarity in what is clearly predicted to be a toward sector. The mismatch within the cloud provides a clue about the magnetic configuration of the source CME, as discussed in section 3.2.

[9] The primary focus of this paper concerns another clue about the magnetic configuration of the source CME. Suprathermal electrons streaming only parallel and not antiparallel to the magnetic field within the cloud give unequivocal evidence that the positive leg of the structure was connected to the Sun and that the negative leg was not. If the negative leg was originally connected and then lost its connection through interchange reconnection, the data imply that open field lines reconnected with the negative leg back at the Sun. The configuration for this interchange reconnection from the interplanetary point of view is illustrated schematically in Figure 3.

[10] The nested cylindrical coils in Figure 3 represent the flux rope structure of the magnetic cloud. The cylindrical force-free model fit by *Webb et al.* [2000] yields a left-handed twist, a leading magnetic field pointing southward, and an axis that tips below the ecliptic plane at an angle $\theta_c = -11^\circ$ at magnetic longitude $\phi_c = 108^\circ$, where $\phi_c = 0^\circ$ points toward the Sun. Other force-free cylindrical model fits give the same twist and similar angular values of $\theta_c = 0^\circ$, $\phi_c = 108^\circ$ (R. P. Lepping, private communication, 2005) and $\theta_c = -13^\circ$, $\phi_c = 93^\circ$ [Lynch et al., 2005]. A dynamic cylindrical model gives the same twist and a similar axis elevation angle of $\theta_c = -10^\circ$ but a different axis longitude of $\phi_c = 162^\circ$ (K. Marubashi, private communication, 2006), discussed further in section 3.2. Although a cylinder is not a realistic shape for a magnetic cloud [e.g., *Suess, 1988; Riley and Crooker, 2004*], most of these cloud properties are probably not highly dependent upon shape and are used here to gain large-scale perspective [cf. *McAllister et al., 2001*]. The axis tilt comes within at least 23° of matching the $\sim 10^\circ$ -upward tilt of the predicted HCS on the coronal map in Figure 2, measured at the heliographic longitude of the cloud ($\sim 145^\circ$). This approximate match and the southward leading field appear to reflect the large-scale dipolar properties of the solar field, consistent with earlier studies [*Bothmer and Rust, 1997; Mulligan et al., 1998; Crooker, 2000*, and references therein]. This match contrasts with the polarity mismatch described above and is discussed further in section 3.2, along with the differences in model values of ϕ_c .

[11] The solar surface in Figure 3 is represented by a photospheric field map from the Wilcox Solar Observatory. Although this kind of map lacks the more accurate details that can be provided by magnetograms from space-based

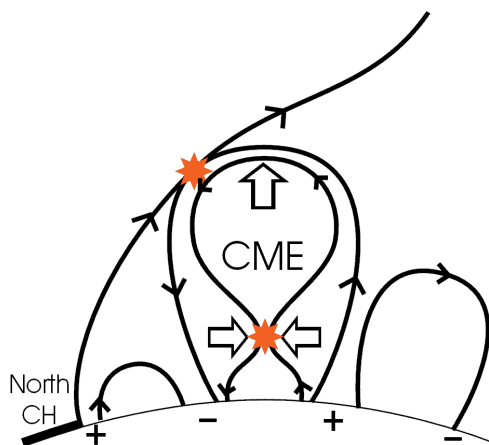


Figure 4. Schematic drawing of the magnetic configuration and reconnection sites (red) of the 12 May 1997 CME. Interchange reconnection high in the corona between open field lines from the northern coronal hole (CH) and closed field lines in the CME acts to open the CME field lines.

measurements, it is suitable for the large-scale analysis discussed here. At this rising phase of solar cycle 23, the northern polar fields were positive (blue contours), and the southern polar fields were negative (red contours). Above the heliographic equator, the map shows the strong bipolar field contours of the active region from which the 12 May CME emerged. The bipolar fields together with the large-scale dipolar fields created a near-quadrupolar structure at the source. The north-pointing arrow between the bipolar contours indicates the pre-erupt orientation of fields in a filament that erupted with the CME. They lay orthogonal to the model cloud axis, in contrast to a statistical tendency toward alignment [e.g., *Zhao and Hoeksema, 1997*], although the left-handed filament chirality matches the cloud twist, as reported by *Webb et al. [2000]*. These parameters are discussed further in section 3.2.

[12] Superposed on the active-region contours in Figure 3 are two shaded areas representing the double-dimming signature seen in images from the Extreme ultraviolet Imaging Telescope (EIT) on the SOHO spacecraft [*Thompson et al., 1998*]. Following *Webb et al. [2000]*, these are treated as the two footpoints of the originally closed flux rope loop comprising the magnetic cloud. *Kahler and Hudson [2001]* raise questions about this kind of association, among them asking why dimmings disappear well before the associated clouds reach 1 AU, where presumably the clouds are still rooted in the Sun. The proposed interchange reconnection, at least in this case, however, may account for the disappearance of the dimming, a possibility foreseen by *Kahler and Hudson [2001]* and discussed further in section 3.1.

[13] The heavy curve in Figure 3 connecting the cylinder to the solar surface represents the core field of the flux rope loop after it lost its connection to the negative footpoint through interchange reconnection with a positive open field line, consistent with the electron data. The field line in what was originally the negative (unsampled) leg of the flux rope acquired positive polarity through the interchange recon-

nection process, even though it locally points toward the Sun, while the field line in the positive (sampled) leg maintained its original polarity and merely became open.

[14] The configuration in Figure 3 immediately raises the question of the source of open field lines feeding into the interchange reconnection site. Although sometimes PFSS models indicate that open fields stem from active regions [e.g., *Neugebauer et al., 2002; Schrijver and DeRosa, 2003; Wang and Sheeley, 2003a*], in this case none was apparent (in three-dimensional (3-D) maps provided by Z. Mikic (private communication, 2004)). The nearest available source of open fields with the required positive polarity was the large reservoir in the northern polar coronal hole, and we assume it was these that fed into the reconnection site.

[15] Figure 4 shows a schematic drawing of the proposed configuration in the corona. Because it is a 2-D rendering of a process with essential 3-D aspects, it fails to show the nonalignment of the active-region bipolar and large-scale dipolar fields, and the implied sequence of reconnection at low and high altitudes should not be treated literally. Nevertheless, the figure captures the essence of the proposed topology. It shows the quadrupolar structure depicted in the well-known breakout model of CME initiation [*Antiochos et al., 1999*], with a flux rope forming through reconnection under the rising CME [e.g., *Lynch et al., 2004*]. In 3-D, however, the structure is not the true quadrupole required by the model dynamics because the neutral line on high-resolution magnetograms forms a peninsula rather than an island (J. A. Linker, private communication, 2005). Moreover, nothing breaks out because there is no overlying dipolar field line confining the emerging flux rope. The field line that reconnects at high altitude is open rather than closed, and its reconnection opens the negative leg of the rising CME.

[16] X-ray images from the Yohkoh Soft X-ray telescope (SXT) show a long-lasting feature that may be a signature of the proposed interchange reconnection. To emphasize its longevity, Figure 5 shows three of these images spaced ~ 3 hours apart. Focused on the upper right-hand (northwestern) quadrant of the Sun, the images prominently display a time sequence of the cusped arcade event associated with the 12 May CME. Cusped arcade events are interpreted as signatures of the reconnection that creates the flux rope, that is, the lower-altitude reconnection illustrated in Figure 4 [e.g., *Shibata et al., 1995; Hundhausen, 1997*]. Fainter but clearly visible in Figure 5 is an arched shape, marked by an arrow in the middle frame, that appears to be at high altitude and extends toward the northern polar region. It is this feature which we interpret as a signature of the higher-altitude interchange reconnection in Figure 4, where the newly closed segment of the originally open field line sunward of the reconnection point represents the illuminated arch. The feature first appeared in an earlier image at 0653 UT and lasted in faint form into the early hours of the next day, consistent with long-lasting interchange reconnection accompanying the flux-rope formation.

[17] We note that the proposed signature of interchange reconnection in Figure 5 is not an uncommon feature. Bright arches that extend from CME sites to coronal hole boundaries have been noted for some time [e.g., *Rust and*

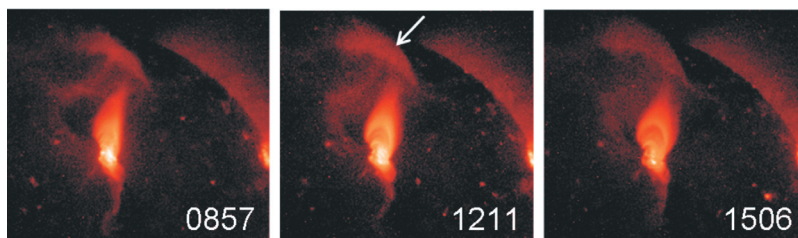


Figure 5. Yohkoh X ray images from three times on 12 May 1997, as marked. The arrow in the middle frame points to the proposed signature of interchange reconnection.

Webb, 1977]. Here we offer a plausible explanation for their occurrence.

3. Discussion

3.1. Interchange Reconnection

[18] The proposed configuration for interchange reconnection in the 12 May event is topologically similar to configurations proposed for two other processes which may be intimately related. The first is interchange reconnection that facilitates the reversal of the solar magnetic field in the course of the solar cycle. *Wang and Sheeley* [2003b] derive nearly the same pattern for the rising phase of the cycle, the same phase in which the May event occurred. The difference between their model and the proposed configuration is that their closed fields are generated by emerging bipoles rather than CMEs, since their model cannot accommodate CME dynamics. Nevertheless, our replication of their topological configuration suggests that their model captures what may be a common reconnection pattern in CMEs.

[19] The second similar configuration is that deduced by *Sterling and Moore* [2001a, 2001b] for what they call “EIT crinkles,” bright patterns that intrude into coronal holes in EIT images. *Sterling and Moore* [2001a, 2001b] identified these patterns in a series of CMEs that occurred on 1–2 May 1998. On the basis of an earlier concept called “tether cutting” [*Sturrock*, 1989; *Moore and Roumeliotis*, 1992], they ascribed the crinkles to “external reconnection” between open and closed field lines at the apex of a rising CME, equivalent to the interchange reconnection described here. In their case the open field lines emerged from a low-latitude coronal hole rather than the polar coronal hole. Because the proposed reconnection site was at the outer boundary of the CME, *Sterling and Moore* [2001a, 2001b] cited EIT crinkles as evidence for the breakout model. Here we suggest that EIT crinkles are just evidence of interchange reconnection and not the breakout model, since any overlying fields that are open do not create a barrier from which a CME must break out, as already mentioned in section 2.

[20] *Sterling and Moore* [2001a, 2001b] also analyzed X-ray images of the 1–2 May 1998 events and showed that the EIT crinkles occurred at the extremities of bright X-ray regions that extended back to the active regions from which the CMEs arose. We suggest that these bright regions, aptly named “anemones” by *Shibata et al.* [1994], can thus be treated as the X-ray signature of interchange reconnection. The X-ray signature, reflecting hotter plasma, would appear along the same magnetic field lines at altitudes higher than the EIT signature. For the 12 May 1997 event, the arched

X-ray feature in Figure 5 may be a perspective view of an anemone, since it occurred at considerably higher latitudes than the 1–2 May 1998 events. Its lower-altitude EUV counterpart appears to have been already identified by *Thompson et al.* [1998]. They show EIT images with brightening at the edge of the northern coronal hole, presumably the legs of loops rooted in what *Sterling and Moore* [2001a, 2001b] would identify as EIT crinkles. These lasted for more than 7 hours, consistent with our supposition that long-lasting interchange reconnection released the negative leg of the CME. EIT brightenings along coronal hole boundaries, like the X-ray features that extend to the boundaries, are not uncommon accompaniments to CMEs (L. Harra, private communication, 2005) and thus comprise likely signatures of frequently associated interchange reconnection.

[21] Regarding the disappearance of the dimming signatures mentioned in section 2, Figure 3 and Figure 4 illustrate how the proposed interchange reconnection may have eliminated the northern dimming region by filling the footprint of the northern leg of the CME with closed field lines. This process meets the expectations of *Kahler and Hudson* [2001] for reconnection of fields outside the CME and contraction of the outer dimming boundary (in addition to the expected contraction of the inner boundary as the arcade under the CME reformed). Dimming in the presumed footprint of the southern leg may have disappeared owing to interchange reconnection, as well, but in a considerably different way, as proposed by *Attrill et al.* [2006]. These authors recently performed a comprehensive study of the dimming and X-ray signatures of the May 1997 event and independently came to the same conclusions regarding the proposed interchange reconnection configuration in Figure 4. They show that dimming in the two regions disappeared at different rates and suggest that the open field lines rooted in the southern region diffused out of the dimming region through interchange reconnection low in the solar atmosphere with small loops in the magnetic carpet. Thus interchange reconnection may be responsible for the disappearance of dimmings either through a return of closed flux or through a dispersal of open flux. These kinds of interchange reconnection may be part of a larger process of global magnetic footpoint circulation as discussed, for example, by *Fisk and Schwadron* [2001].

3.2. Solar Magnetic Field Imprint and Model Implications

[22] Section 2 notes two ways in which the 15 May 1997 ICME appeared to carry the imprint of the dipolar component of the solar magnetic field (a southward leading field

and cloud axis alignment with the HCS) and one way in which it did not (the mismatch of the polarity of the cloud leg with the sector polarity). Moreover, the cloud did not appear to carry the imprint of the higher-order filament fields, since its axis was orthogonal to the filament axis. These mixed signals may reflect a mix of elements from the breakout model of CMEs, with its focus on quadrupolar structure, as discussed in section 2, and models which focus on the dipolar structure of flux-rope formation through reconnection of helmet streamer field lines [e.g., *Lin and Forbes*, 2000; *Low and Zhang*, 2002; *Linker et al.*, 2003], especially because all of these models, including tether cutting, are closely related [e.g., *Isenberg et al.*, 1993; *Lin et al.*, 2001; *Lynch et al.*, 2004]. On the other hand, Figure 3 suggests a more specific geometrical explanation described below in terms of where the spacecraft intersected the flux rope loop.

[23] The configuration of the magnetic field, of the dimmings, and of the preeruption filament axis at the CME site in Figure 3 and the orientation of the bright arcade in Figure 5 consistently predict the formation of a left-handed flux rope with a north-pointing axis, tilted slightly to the east, and with predominantly eastward leading fields. Studies that use this kind of prediction and assume little change in flux rope orientation as the CME moves out into the heliosphere have been reasonably successful in matching magnetic cloud properties [e.g., *Bothmer and Rust*, 1997; *Zhao and Hoeksema*, 1997; *Crooker et al.*, 1998; *McAllister et al.*, 2001]. In this case, however, the observed cloud, with its southward leading fields and east-pointing axis, lay essentially orthogonal to the predicted one. The only match with a predictive parameter was the near-alignment of the cloud axis with the HCS, and this parameter is an outlier in the sense that it does not agree with those listed above. *Webb et al.* [2000] point out that the flux rope may have rotated counterclockwise as it rose, since the erupting filament, presumably threading the rope [e.g., *Lin and Forbes*, 2000; *Low and Zhang*, 2002], was observed to do so.

[24] An alternative possibility is that the flux rope axis maintained a north-south orientation, reflecting a match with the filament axis rather than the HCS, but that the spacecraft encountered its southern leg rather than the apex of the loop. For flux rope loops that leave the Sun with north-south axes, that orientation can be maintained only at the apex of the loop, while the legs will tend to stretch out along the Parker spiral. Figure 3 attempts to convey this geometry, where the position of the cylindrical form illustrating the flux rope structure, along the southern leg of the loop, sunward of the loop's apex, indicates the proposed site of spacecraft encounter. Consistent with this view, the cloud axis longitude ϕ_c in the leg location agrees better with the more realistic dynamic model fit (162°) compared to the force-free fits (93° , 108°) discussed in section 2, where the latter seem to mistakenly imply encounter with the apex. Even better agreement ($\phi_c = 139^\circ$ (K. Marubashi, private communication, 2006)), in the sense of being closer to the Parker spiral, is obtained with the dynamic curved cylindrical model of *Marubashi* [1997, 2002], approximated by a torus. Encounter with the southern leg is also consistent with the observed mismatch between the polarity of the cloud leg and the polarity of the sector in which it was

imbedded. This mismatch reflects the near-quadrupolar structure at the source, where the footpoint of the southern leg has a polarity opposite that of the southern dipolar field (Figure 3).

4. Conclusions

[25] Using observations of suprathermal electrons in the 15 May 1997 magnetic cloud at 1 AU, we have remotely identified what appear to be signatures of CME-associated interchange reconnection on the Sun in X-ray and EUV observations. These signatures are global in nature, spanning from the active-region source to the polar coronal hole. Since global-scale coronal activity is commonly noted in association with CMEs, it may be that signatures of interchange reconnection are commonly observed but until now have not been recognized as such. Further case studies are needed to test this possibility.

[26] The mixed signatures of the imprint of the solar magnetic field on the 15 May 1997 magnetic cloud were at first surprising in view of the isolation and relative simplicity of the event. Analysis of the cloud parameters in the context of the heliospheric magnetic field and the configuration of the source region, however, suggest that the mixed signatures arose from straightforward geometrical constraints.

[27] **Acknowledgments.** This material is based in part upon work supported by the National Science Foundation under grant ATM-0553397 and under agreement ATM-012950 of the STC program, which funds the Center for Integrated Space Weather Modeling (CISM), and by NASA under grant NNG05GD97G. The authors thank S. W. Kahler and A. C. Sterling for helpful comments.

[28] Zuyin Pu thanks the reviewers for their assistance in evaluating this paper.

References

- Antiochos, S. K., C. R. DeVore, and J. A. Klimchuk (1999), A model for solar coronal mass ejections, *Astrophys. J.*, *510*, 485–493.
- Arge, C. N., J. G. Luhmann, D. Odstrcil, C. J. Schrijver, and Y. Li (2004), Stream structure and coronal sources of the solar wind during the May 12th, 1997 CME, *J. Atmos. Terr. Phys.*, *66*, 1295–1309.
- Attrill, G., M. S. Nakwacki, L. K. Harra, L. vanDriel-Gesztelyi, C. H. Mandrini, S. Dasso, and J. Wang (2006), Using the evolution of coronal dimming regions to probe the global magnetic field topology, *Sol. Phys.*, in press.
- Bothmer, V., and D. M. Rust (1997), The field configuration of magnetic clouds and the solar cycle, in *Coronal Mass Ejections*, *Geophys. Monogr. Ser.*, vol. 99, edited by N. U. Crooker, J. A. Joselyn, and J. Feynman, pp. 137–146, AGU, Washington, D. C.
- Burlaga, L. F. (1991), Magnetic clouds, in *Physics of the Inner Heliosphere II*, edited by R. Schwenn and E. Marsch, pp. 1–22, Springer, New York.
- Crooker, N. U. (2000), Solar and heliospheric geoeffective disturbances, *J. Atmos. Sol. Terr. Phys.*, *62*, 1071–1085.
- Crooker, N. U. (2005), ICME-CME connections: Outstanding questions, in *Solar Wind Eleven*, edited by B. Fleck and T. H. Zurbuchen, *Eur. Space Agency Spec. Publ.*, *ESA SP 592*, 289–295.
- Crooker, N. U., et al. (1998), Sector boundary transformation by an open magnetic cloud, *J. Geophys. Res.*, *103*, 26,859–26,868.
- Crooker, N. U., J. T. Gosling, and S. W. Kahler (2002), Reducing heliospheric magnetic flux from coronal mass ejections without disconnection, *J. Geophys. Res.*, *107*(A2), 1028, doi:10.1029/2001JA000236.
- Fisk, L. A., and N. A. Schwadron (2001), The behavior of the open magnetic field of the Sun, *Astrophys. J.*, *560*, 425–438.
- Gosling, J. T., D. N. Baker, S. J. Bame, W. C. Feldman, and R. D. Zwickl (1987), Bidirectional solar wind electron heat flux events, *J. Geophys. Res.*, *92*, 8519–8535.
- Gosling, J. T., S. J. Bame, D. J. McComas, and J. L. Phillips (1990), Coronal mass ejections and large geomagnetic storms, *Geophys. Res. Lett.*, *17*, 901–904.

- Gosling, J. T., J. Birn, and M. Hesse (1995), Three-dimensional magnetic reconnection and the magnetic topology of coronal mass ejection events, *Geophys. Res. Lett.*, *22*, 869–872.
- Hundhausen, A. J. (1997), Coronal mass ejections, in *Cosmic Winds and the Heliosphere*, edited by J. R. Jokipii, C. P. Sonett, and M. S. Giampapa, pp. 259–296, Univ. of Ariz. Press, Tucson.
- Isenberg, P. A., T. G. Forbes, and P. Demoulin (1993), Catastrophic evolution of a force-free flux rope: A model for eruptive flares, *Astrophys. J.*, *417*, 368–386.
- Kahler, S. W., and H. S. Hudson (2001), Origin and development of transient coronal holes, *J. Geophys. Res.*, *106*, 29,239–29,248.
- Kahler, S. W., N. U. Crooker, and J. T. Gosling (1999), The polarities and locations of interplanetary coronal mass ejections in large interplanetary magnetic sectors, *J. Geophys. Res.*, *104*, 9919–9924.
- Lepping, R. L., et al. (1995), The Wind magnetic field investigation, *Space Sci. Rev.*, *71*, 207–229.
- Lin, J., and T. G. Forbes (2000), Effects of reconnection on the coronal mass ejection process, *J. Geophys. Res.*, *105*, 2375–2392.
- Lin, J., T. G. Forbes, and P. A. Isenberg (2001), Prominence eruptions and coronal mass ejections triggered by newly emerging flux, *J. Geophys. Res.*, *106*, 25,053–25,074.
- Lin, R. P., et al. (1995), A three-dimensional plasma and energetic particle investigation for the Wind spacecraft, *Space Sci. Rev.*, *71*, 125–153.
- Linker, J. A., Z. Mikic, V. R. Lionello, and P. Riley (2003), Flux cancellation and coronal mass ejections, *Plasma Phys.*, *10*, 1971–1978.
- Linker, J. A., Z. Mikic, V. Titov, R. Lionello, and P. Riley (2005), Modeling active region coronal mass ejections, *Eos Trans. AGU*, *86*(18), Jt. Assem. Suppl., Abstract SH54B-05.
- Liu, Y. (2004), Photospheric magnetic field observations during the May 12, 1997 CME and their implications for modeling that event, *J. Atmos. Terr. Phys.*, *66*, 1283–1293.
- Low, B. C., and M. Zhang (2002), The hydromagnetic origin of the two dynamical types of solar coronal mass ejections, *Astrophys. J.*, *564*, L53–L56.
- Lynch, B. J., S. K. Antiochos, P. J. MacNeice, T. H. Zurbuchen, and L. A. Fisk (2004), Observable properties of the breakout model for coronal mass ejections, *Astrophys. J.*, *617*, 589–599.
- Lynch, B. J., J. R. Gruesbeck, T. H. Zurbuchen, and S. K. Antiochos (2005), Solar cycle–dependent helicity transport by magnetic clouds, *J. Geophys. Res.*, *110*, A08107, doi:10.1029/2005JA011137.
- Marubashi, K. (1997), Interplanetary magnetic flux ropes and solar filaments, in *Coronal Mass Ejections, Geophys. Monogr. Ser.*, vol. 99, edited by N. U. Crooker, J. A. Joselyn, and J. Feynman, pp. 147–156, AGU, Washington, D. C.
- Marubashi, K. (2002), Interplanetary flux ropes, *J. Commun. Res. Lab.*, *49*, 41–59.
- McAllister, A. H., S. F. Martin, N. U. Crooker, R. P. Lepping, and R. J. Fitzenreiter (2001), A test of real-time prediction of magnetic cloud topology from solar signatures, *J. Geophys. Res.*, *106*, 29,185–29,194.
- Moore, R. L., and G. Roumeliotis (1992), Triggering of eruptive flares - destabilization of the preflare magnetic field configuration, in *Eruptive Solar Flares, Proc. IAU*, vol. 133, edited by Z. Svestka, B. V. Jackson, and M. E. Machado, pp. 69–78, Springer, New York.
- Mulligan, T., C. T. Russell, and J. G. Luhmann (1998), Solar cycle evolution of the structure of magnetic clouds in the inner heliosphere, *Geophys. Res. Lett.*, *25*, 2959–2963.
- Neugebauer, M., P. C. Liewer, E. J. Smith, R. M. Skoug, and T. H. Zurbuchen (2002), Sources of the solar wind at solar activity maximum, *J. Geophys. Res.*, *107*(A12), 1488, doi:10.1029/2001JA000306.
- Odstroil, D., P. Riley, and X. P. Zhao (2004), Numerical simulation of the 12 May 1997 interplanetary CME event, *J. Geophys. Res.*, *109*, A02116, doi:10.1029/2003JA010135.
- Odstroil, D., V. J. Pizzo, and C. N. Arge (2005), Propagation of the 12 May 1997 interplanetary coronal mass ejection in evolving solar wind structures, *J. Geophys. Res.*, *110*, A02106, doi:10.1029/2004JA010745.
- Plunkett, S. P., et al. (1998), LASCO observations of an Earth-directed coronal mass ejection on May 12, 1997, *Geophys. Res. Lett.*, *25*, 2477–2480.
- Riley, P., and N. U. Crooker (2004), A kinematic treatment of CME evolution in the solar wind, *Astrophys. J.*, *600*, 1035–1042.
- Rust, D. M., and D. F. Webb (1977), Soft X ray observations of large-scale coronal active region brightenings, *Sol. Phys.*, *54*, 403–417.
- Schrijver, C. J., and M. L. DeRosa (2003), Photospheric and heliospheric magnetic fields, *Sol. Phys.*, *212*, 165–200.
- Suess, S. T. (1988), Magnetic clouds and the pinch effect, *J. Geophys. Res.*, *93*, 5437–5445.
- Shibata, K., et al. (1994), A gigantic coronal jet ejected from a compact active region in a coronal hole, *Astrophys. J.*, *431*, L51–L53.
- Shibata, K., et al. (1995), Hot-plasma ejections associated with compact-loop solar flares, *Astrophys. J.*, *451*, L83–L85.
- Shodhan, S., et al. (2000), Counterstreaming electrons in magnetic clouds, *J. Geophys. Res.*, *105*, 27,261–27,268.
- Sterling, A. C., and R. L. Moore (2001a), Internal and external reconnection in a series of homologous solar flares, *J. Geophys. Res.*, *106*, 25,227–25,238.
- Sterling, A. C., and R. L. Moore (2001b), EIT crinkles as evidence for the breakout model of solar eruptions, *Astrophys. J.*, *560*, 1045–1057.
- Sturrock, P. A. (1989), The role of eruption in solar flares, *Sol. Phys.*, *121*, 387–397.
- Thompson, B. J., S. P. Plunkett, J. B. Gurman, J. S. Newmark, O. C. St. Cyr, and D. J. Michels (1998), SOHO/EIT observations of an Earth-directed coronal mass ejection on May 12, 1997, *Geophys. Res. Lett.*, *25*, 2465–2468.
- Wang, Y.-M., and N. R. Sheeley Jr. (2003a), The solar wind and its magnetic sources at sunspot maximum, *Astrophys. J.*, *587*, 818–822.
- Wang, Y.-M., and N. R. Sheeley Jr. (2003b), On the topological evolution of the coronal magnetic field during the solar cycle, *Astrophys. J.*, *599*, 1404–1417.
- Webb, D. F., et al. (2000), The origin and development of the May 1997 magnetic cloud, *J. Geophys. Res.*, *105*, 27,251–27,259.
- Zhao, X.-P., and J. T. Hoeksema (1997), Is the geoeffectiveness of the 6 January 1997 CME predictable from solar observations?, *Geophys. Res. Lett.*, *24*, 2965–2968.

N. U. Crooker, Center for Space Physics, Boston University, 725 Commonwealth Avenue, Boston, MA 02215, USA. (crooker@bu.edu)

D. F. Webb, Air Force Research Laboratory/VSBXS, 27 Randolph Road, Hanscom AFB, MA 01731-3010, USA.